3 Mechanics of land subsidence due to fluid withdrawal, by Joseph F. Poland and Working Group

3.1 INTRODUCTION

The three types of fluid withdrawal by man that have caused noticeable subsidence under favorable geologic conditions are (1) the withdrawal of oil, gas, and associated water, (2) the withdrawal of hot water or steam for geothermal power, and (3) the withdrawal of ground water. Each of the three types of withdrawal has produced maximum subsidence of the same order of magnitude. For example, the best known example of oil-field subsidence is the Wilmington oil field in Los Angeles County, California, which has experienced 9 metres of subsidence (Mayuga and Allen, 1969); the withdrawal of hot water for geothermal power at Wairakei, New Zealand, has produced 6-7 metres of subsidence (case history 9.9); and the withdrawal of ground water has produced 9 metres of subsidence in both Mexico City, Mexico, and the San Joaquin Valley of California, USA. (See Table 1.1 and case histories 9.8 and 9.13.) In this guidebook we are concerned with subsidence due to ground-water withdrawal but, regardless of the nature of the fluid removed, the principles involved are the same.

A common understanding of terms is important in discussing the mechanics of land susidence. The reader is referred to three U.S. Geological Survey publications for the definition of many pertinent terms: Water-Supply Paper 494 (Meinzer, 1923) was one of the first comprehensive attempts to define terms used in ground-water studies and has been a much used reference work for the past half century; Water-Supply Paper 1988 (Lohman and others, 1972) contains revised and clarified definitions of selected ground-water terms and stresses the use of consistent units in ground-water flow equations; Water-Supply Paper 2025 (Poland, Lofgren, and Riley, 1972) is a glossary of selected terms useful in studies of the mechanics of aquifer systems and land subsidence due to fluid withdrawal. Principal terms will be defined briefly in this chapter or in an appended glossary, Appendix D.

Figure 3.1 illustrates the terminology for subdivisions of a ground-water reservoir as used in this manual. Case 1, on the left, depicts, from top to bottom, the land surface, a water table, and an unconfined aquifer that functions as an hydraulic unit, a confining bed that functions as a major hydraulic separator; a confined aquifer system that functions approximately as an hydraulic unit; and relatively impermeable bedrock at the base. Case 2 depicts, from top to bottom, the land surface; a water table associated with a semiconfined aquifer system; a confining bed; a confined aquifer system; a second confining bed; a saltwater confined aquifer system; and relatively impermeable bedrock at the base.

Attention is directed to the confined aquifer system that occurs in both cases. Note in particular that aquitards which occur within an hydraulic unit are distinct from a confining bed that serves as an hydraulic separator. For illustrative purposes, the system includes two aquitards (fine-grained compressible interbeds) and three aquifers. Because the aquitards are highly compressible compared to the clastic sand or sand and gravel of the aquifers, they determine by their number and thickness the susceptibility of the aquifer system to compaction in response to increase in stress. In highly compressible confined systems that have experienced several metres of manmade compaction, several tens of aquitards may be interbedded with the aquifers. For example, the microlog of a well drilled through a 400-metre thickness of the confined system on the west side of the San Joaquin Valley, California, displayed 60 aquitards with individual thicknesses ranging from 0.6 m to 15 m and averaging 4.5 m.

In contrast to the large number of aquitards subject to compaction in the San Joaquin Valley, in Mexico City most of the 9 m of compaction has occurred in the top 50 m below land surface, chiefly in two very highly compressible silty clay beds 25-30 and 5-10 m thick. In the upper thicker clay the void ratio averages about 7 and the porosity about 88 per cent; in the lower clay the void ratio averages 4-5 and the porosity about 82 per cent. Figueroa-Vega concludes (case history 9.8, Table 9.8.5) from comparison of casing protrusion and subsidence for 1970-73 that about 75 per cent of the total subsidence was due to compaction of the clayey strata in the top 50 m, and the remainder to compression of the underlying aquifer which is several hundred m thick.

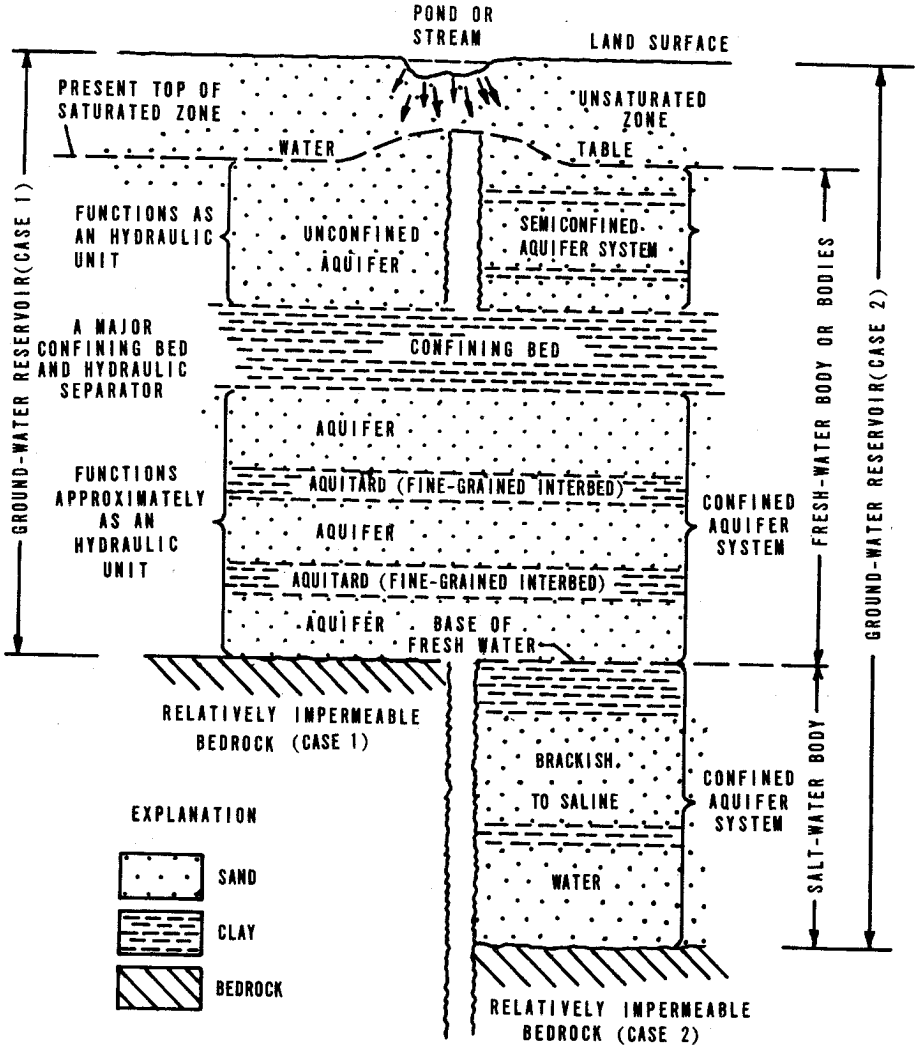

Figure 3.1 Diagram showing terminology for a ground-water reservoir and subdivisions thereof.

In order to count the number and individual thicknesses of the aquitards (or of the aquifers) as displayed in a geophysical bore-hole log, an arbitrary vertical reference, line is drawn on the log. Intervals where the resistivity log lies to the left of the reference line define aquitards; intervals where the resistivity log lies to the right of the reference line define aquifers. Where precisely to draw the reference line becomes a matter of personal judgment. Among the geophysical logs available from oil-field service companies, the microlog of Schlumberger gives considerably more lithologic detail than do the logging devices using a normal electrode configuration. Of these, the short normal with an electrode spacing of about 0.4 metre gives the best detail on thin aquitards.

Figure 9.3.2 is a vertical section of the confined aquifer system beneath Venice, Italy. Using the electric logs and core descriptions from deep test boreholes, the authors of the case history on Venice have divided the confined system into six principal aquifers and a considerable number of aquitards.

3.2 THEORY OF AQUIFER-SYSTEM COMPACTION

In 1925, O. E. Meinzer (Meinzer and Hard, 1925, p. 91) recognized that an artesian aquifer (the Dakota Sandstone) was compressed when the artesian head was decreased. He stated (p. 92) that the overburden pressure of all beds above the confined Dakota aquifer was supported partly by

the fluid pressure at the top of the Dakota and partly by the sandstone itself (grain-to-grain load). He concluded that the grain-to-grain load on the Dakota aquifer at Ellendale, North Dakota, had increased about 50 per cent because of the decline of artesian head.

Meinzer (1928), in a classic paper, discussed the compressibility and elasticity of artesian aquifers in detail. He cited evidence for compressibility and elasticity derived from laboratory tests and from field evidence for confined aquifers and for large artesian basins, notably the Dakota artesian basin. He concluded (p. 289):

> . . . artesian aquifers are apparently all more or less compressible and elastic though they differ widely in the degree and relative importance of these properties. In general the properties of compressibility and elasticity are of the most consequence in aquifers that have low permeability, slow recharge, and high head. In many aquifers these properties are evidently important in supplying water not only by permanent reduction of storage but also by temporary reduction that is replenished when the wells are shut down or during the season of minimum use."

He recognized that water withdrawn from storage was released both by compression of the aquifer and by expansion of the water and that reduction of storage--compression--may be permanent (inelastic) as well as elastic (recoverable).

The next milestone in the understanding of the manner in which artesian aquifers release water from storage was the development by Theis (1935), through analogy with the mathematical theory of heat conduction, of an equation for the non-steady-state flow of ground water to a discharging well. This equation, which for the first time introduced the elements of time and the coefficient of storage (S), subsequently has become the foundation of quantitative ground-water hydrology. Following development of this equation, Theis (1938, p. 894) defined the coefficient of storage as ". . . the volume of water, measured in cubic feet, released from storage in each column of the aquifer having a base one foot square and a height equal to the thickness of the aquifer, when the water table or other piezometric surface is lowered one foot."

Jacob (1940) postulated that when water is removed from and pressure is decreased in an elastic artesian aquifer, stored water is derived from expansion of the confined water, compression of the aquifer, and compression of the adjacent and included clay beds. He concluded that the third source is probably the chief one in the usual case, and he stated (p. 574), ". . . because of the low permeability of the clays (or shales) there is a time lag between the lowering of pressure within the aquifer and the appearance of that part of the water which is derived from storage in those clays (or shales)."

In the field of soil mechanics, Karl Terzaghi (1925; Terzaghi and Peck, 1967) developed the theory of primary one-dimensional consolidation of clays that has served as the basis for solution of most practical soil mechanics and settlement problems in the past half century. This theory commonly is used to estimate the magnitude and rate of settlement or compaction that will occur in fine-grained clayey deposits under a given change in load (stress). According to the theory, compaction results from the slow escape of pore water from the stressed deposits, accompanied by a gradual transfer of stress from the pore water to the granular structure of the deposits. In developing his consolidation theory in 1925, Terzaghi also introduced the basic principle of effective stress that

$$p' = p - u_w, \qquad (3.1)$$

where

p' = effective stress (effective overburden pressure or grain-to-grain load),
p = total stress (geostatic pressure), and
u_w = pore pressure (fluid pressure or neutral stress).

This was the same year that 0. E. Meinzer (Meinzer and Hard, 1925) recognized the principle of effective stress in compression of artesian aquifers.

The application of the time-consolidation theory of soil mechanics to explain the theory of aquifer-system compaction has been summarized lucidly by Riley (1969), as follows:

> "The well-known hydrodynamic (Terzaghi) theory of soil consolidation can provide a semi-quantitative explanation for the phenomenon of repeated permanent compaction during successive cycles of loading and unloading through about the same stress range. In the

context of this problem a central tenet of consolidation theory states that an increase in stress applied to a "clay" stratum (aquitard) becomes effective as a compressive grain-to-grain load only as rapidly as the heads (pore pressures) in the aquitard can decay toward equilibrium with the head in the adjacent aquifer(s). Because of the low permeability and relatively high compressibility of the interbedded aquitards, the consolidation (compaction) of a multi-layered aquifer system in response to increased applied stress is a strongly time-dependent process, and complete or "ultimate" consolidation is not attained until a steady-state vertical distribution of head exists throughout the aquifer system. Transient heads in the aquitards higher than those in the adjacent aquifers (termed residual excess pore pressures) are a direct measure of the remaining primary consolidation that will ultimately occur under the existing stress. When pore-pressure equilibrium is attained throughout the aquitard, it is said to be 100 per cent consolidated for the prevailing stress and no further permanent compaction will occur if the same stress is repeatedly removed and reapplied. The possible role of secondary, or nonhydrodynamic, consolidation in aquifer-system compaction is not well-known, but is assumed in this discussion to be minor.)

"For a single homogeneous aquitard, bounded above and below by aquifers in which the head is instantaneously and equally lowered, the time, t, required to attain any specified dissipation of average excess pore pressure is a direct function of: (1) the volume of water that must be squeezed out of the aquitard in order to establish the denser structure required to withstand the increased stress, and (2) the impedance to the escape of this water. The product of these two parameters constitutes the aquitard time constant. For a specified stress increase, the volume of water is determined by the volume compressibility m_v, of the aquitard, the compressibility, β_w, of the water, and the thickness, b′, of the aquitard. The impedance is determined by vertical permeability, K′, and thickness of the aquitard. Thus, the required time, is a function of the time constant, τ, where

$$\tau = \frac{S'_s(b'/2)^2}{K'} \qquad (3.2)$$

and where S'_S is the specific storage of the aquitard, defined as

$$S'_S = S'_{Sk} + S_{sw} \qquad (3.3)$$

in which

$$S'_{sk} = m_v\gamma_w = \frac{\Delta b'}{b'\Delta h_a} \qquad (3.4)$$

and

$$S_{sw} = n\beta_w\gamma_w \qquad (3.5)$$

S'_{sk} is the component of specific storage due to compressibility of the aquitard, S is the component due to the compressibility of water, h_a is the average head in the aquitard, n is the porosity, and γ_w is the unit weight of water. For consolidating aquitards $S'_{sk} >>> S_{sw}$.

"For convenience, it is customary to define a dimensionless time factor, T, such that

$$T = \frac{t}{\tau'} \qquad (3.6)$$

when T equals unity, t equals the time constant. The degree of consolidation U%, at any time, t, is then expressed as a function of T, the form of the functional relation being determined by the initial conditions of the problem. For the commonly used time-consolidation functions, U% is somewhat more than 90 per cent when T is unity. Detailed development of the time-consolidation theory summarized above may be found in Scott (1963, p. 162-197.)"

3.3 ANALYSIS OF STRESSES CAUSING SUBSIDENCE

3.3.1 Types of stresses

As discussed by Lofgren (1968), three types of stresses are involved in the compaction of an aquifer system:

> "These are closely interrelated, yet of such different nature that a clear distinction is of utmost importance. The first of these is a gravitational stress, caused by the effective weight of overlying deposits, which is transmitted downward through the grain-to-grain contacts in the deposits. The second, a hydrostatic stress due to the weight of the interstitial water, is transmitted downward through the water. The third is a dynamic seepage stress exerted on the grains by the viscous drag of vertically moving interstitial water. The first and third are additive in their effect and together comprise the grain-to-grain stress which effectively changes the void ratio and mechanical properties of the deposit; it is commonly known as the "effective stress." The second type of stress, although it tends to compress each individual grain, has virtually no tendency to change the void ratio of the deposit and is referred to as a neutral stress.
> "Of the various methods used in analyzing the effect of these stresses in a compacting aquifer system (Taylor, 1948, p. 203), only two are considered here. Although they vary in their conceptual approach, these methods give the same mathematical results and can be used to check one another. The classical method, the approach most often used in practical soil-mechanics problems, considers the geostatic load, or combined total weight of grains and water in the system, and the neutral, or hydrostatic, stress. The second method considers the static gravitational stress of the grains, which comprises their true weight above the water table and submerged (buoyed) weight below the water table, and the vertical seepage stresses that may exist in the system. Inasmuch as changes in the effective grain-to-grain stress (both gravitational and stress due to seepage) are directly responsible for the compaction of the deposits and are directly related to changes in head in an aquifer system, this second approach has proved the simplest and clearest in our subsidence investigation."

The definition of seepage stress as a net cumulative difference in hydraulic head is a powerful and useful concept, although the interpretation of seepage stress as being caused by viscous drag may be found to be subject to question in the future. For further discussion of this issue, the reader is referred to Helm (1978) and Helm (1980).

The diagram in Figure 3.2 illustrates the stresses acting at the interface between an artesian aquifer and the overlying confining bed. If we assume that the total load, p, exerted on the aquifer is constant and u_w is reduced as a result of pumping, the load borne by the skeleton of the aquifer, p', is increased by an equal amount. If the artesian head is drawn down to the base of the confining bed (u_w=O), the effective stress, p', on the aquifer skeleton equals the geostatic pressure p.

The idealized pressure diagram of Figure 3.3 utilizes the classical method to illustrate the stresses that cause subsidence. (Also see Poland and Davis, 1969, Figures 1-3.) For the sake of simplicity, pressure is expressed in terms of the height of an equivalent column of water. The geostatic pressure (total stress), p, of sediments and water at some plane of reference below the water table equals the unit weight of moist sediments above the water table, γ_m, times their thickness, plus the unit weight of saturated sediments below the water table, γ, times their thickness. If we assume an average porosity, n, of 40 per cent, an average specific gravity, G, of 2.70 for the grains, an average specific retention, r_s, of 0.20 for the moisture contained above the water table, and let the unit weight of water be unity, then, γ_m equals 1.8 metres of water per metre of thickness:

$$\gamma_m = [G(1-n) + r_s]\gamma_w, \text{ or } [2.7(1-0.4) + 0.20]1 = 1.8, \quad (3.7)$$

and γ= 2.0 metres of water per metre of thickness:

$$\gamma = [G(1-n) + n]\gamma_w, \text{ or } [2.7(1-0.4) + 0.4]1 = 2.0. \quad (3.8)$$

Thus the geostatic pressure at depth $z_1 + z_2$ (figure 3.3) is

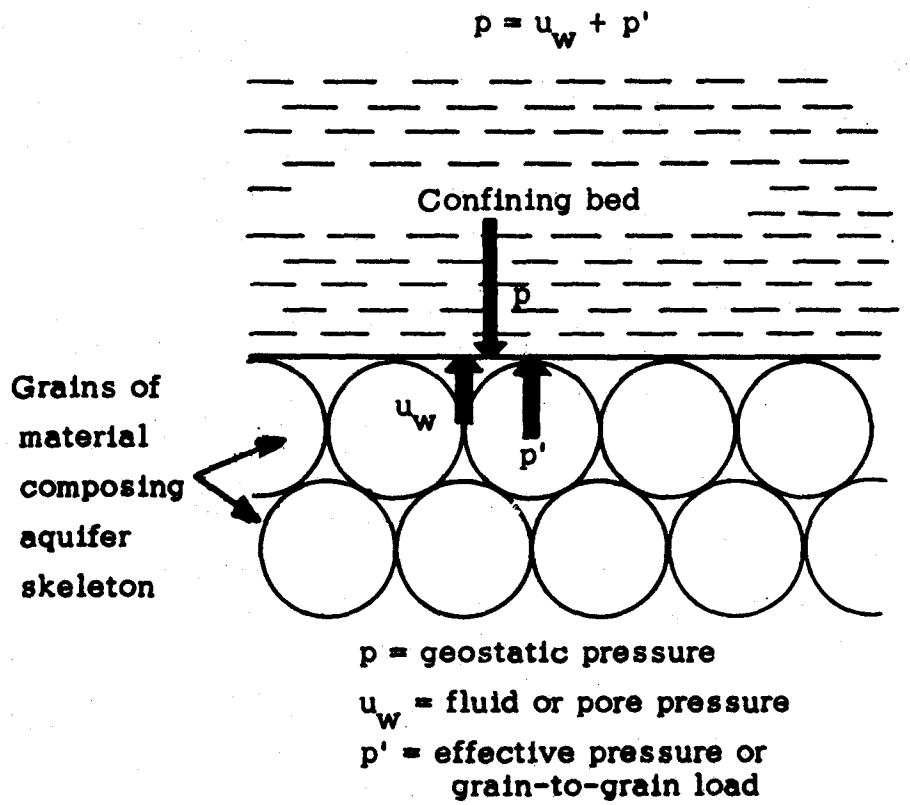

Figure 3.2 Diagrammatic view of stresses acting at interface between artesian aquifer and confining bed (modified from Ferris, Knowles, Brown, and Stallman, 1962, p. 79).

$$p = z_1\gamma_m + z_2\gamma = (50 \times 1.8) + (450 \times 2.0) = 990 \text{ metres of water} \quad (3.9)$$

(a column of water 1 metre high exerts a pressure of 0.1 kg cm^{-2} on its base)

The lowering of artesian head in a confined aquifer system, for example, from depth (Z_1) to (Z_3) in Figure 3.3, does not change the geostatic pressure appreciably. Therefore, the increase in effective stress in the confined aquifers is equal to the decrease in fluid pressure. The compaction in these is immediate and is chiefly recoverable if fluid pressure is restored, but usually it is small.

On the other hand, in the aquitards (fine-grained interbeds) and confining beds, which have low vertical permeability and high specific storage under virgin stressing, the vertical escape of water and the adjustment of pore pressures is slow and time-dependent. Hence, the stress increase applied at the aquifer-aquitard boundaries by the head decline in the confined aquifers becomes effective in these fine-grained beds only as rapidly as pore pressures decay toward equilibrium with those in adjacent aquifers. (See dashed pore-pressure lines of Figure 3.3; where u_t represents the excess pore pressure at time t.) Attainment of pore-pressure equilibrium (dotted lines) may take months or years; the time varies directly as the specific storage and the square of the draining thickness and inversely as the vertical hydraulic conductivity of the aquitard or the confining bed.

Although not illustrated in Figure 3.3, it is readily apparent that increase of fluid pressure from a steady-state condition decreases effective stress and causes expansion of the pressurized sediments (as in subsidence control and underground waste disposal). Fluid pressure cannot exceed geostatic pressures without causing uplift of the overburden.

The stress relations of Figure 3.3 serve to illustrate the principle of effective stress, but do not emphasize the importance of net difference of hydraulic head in causing compaction. Actually, the downward hydraulic gradient developed across the confining bed by the head decline in the confined system induces downward movement of water through the pores that exerts a viscous drag on the clay particles. The stress so exerted on the particles in the confining bed in the direction of flow is a seepage stress.

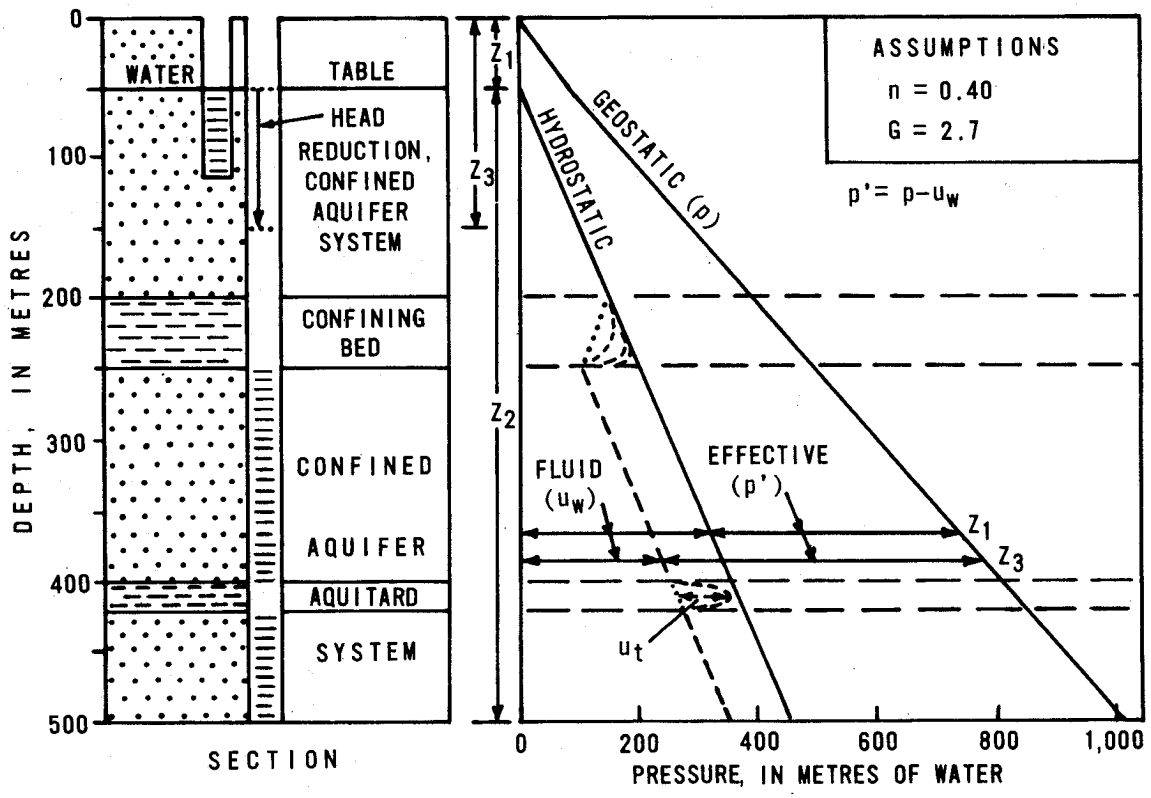

Figure 3.3 Pressure diagram for an unconfined aquifer and a confined aquifer system; head reduction in the confined system only.

3.3.2 Computation of stress change

It is quantitatively convenient in treating complex aquifer systems to compute effective stresses and stress changes in terms of gravitational stress and the vertical normal component of seepage stress, which are algebraically additive. The following brief discussion is summarized from Lofgren (1968) and Poland and others (1975).

Diagram A of Figure 3.4 illustrates part of a confined aquifer system containing an aquitard, overlain by a confining bed and an unconfined aquifer. The water table and the potentiometric surface of the confined system are initially at the same depth; hence, fluid pressure at all depths is hydrostatic. All beds and surfaces within the vertical column are assumed to be horizontal. If we assume the same parameters as for Figure 3.3, and let the unit weight of water be unity, then the effective unit weight of moist deposits above the water table, γ_m, equals 1.8 metres of water per metre of thickness:

$$\gamma_m = [G(1-n) + r_s]\gamma_w, \text{ or } [2.7(1-0.4) + 0.20]1 = 1.8 \qquad (3.7)$$

Also, the effective submerged, or buoyant, unit weight of saturated deposits, γ_b, equals one metre of water per metre of thickness:

$$\gamma_b = (1-n)\,(G-1)\gamma_w, \text{ or } (1-0.4)\,(2.7-1)1 = 1.0 \qquad (3.10)$$

If these gravitational stresses Are expressed in metres of water (one metre of water is equivalent to 0.1 kg cm^{-2}), they can be added directly to hydraulic stresses.

Vectors to the right of diagram A (Figure 3.4) represent the two components of effective gravitational stress at three depths. At the 400-metre depth, for example, the stress due to the unsaturated deposits, s, equals 200 metres of thickness times 1.8, or 360 metres of water; the stress due to the buoyant weight of submerged deposits, b, equals 200 x 1.0, or 200 metres of water. The sum of s + b, 560 metres of water, is the grain-to-grain stress at this plane of

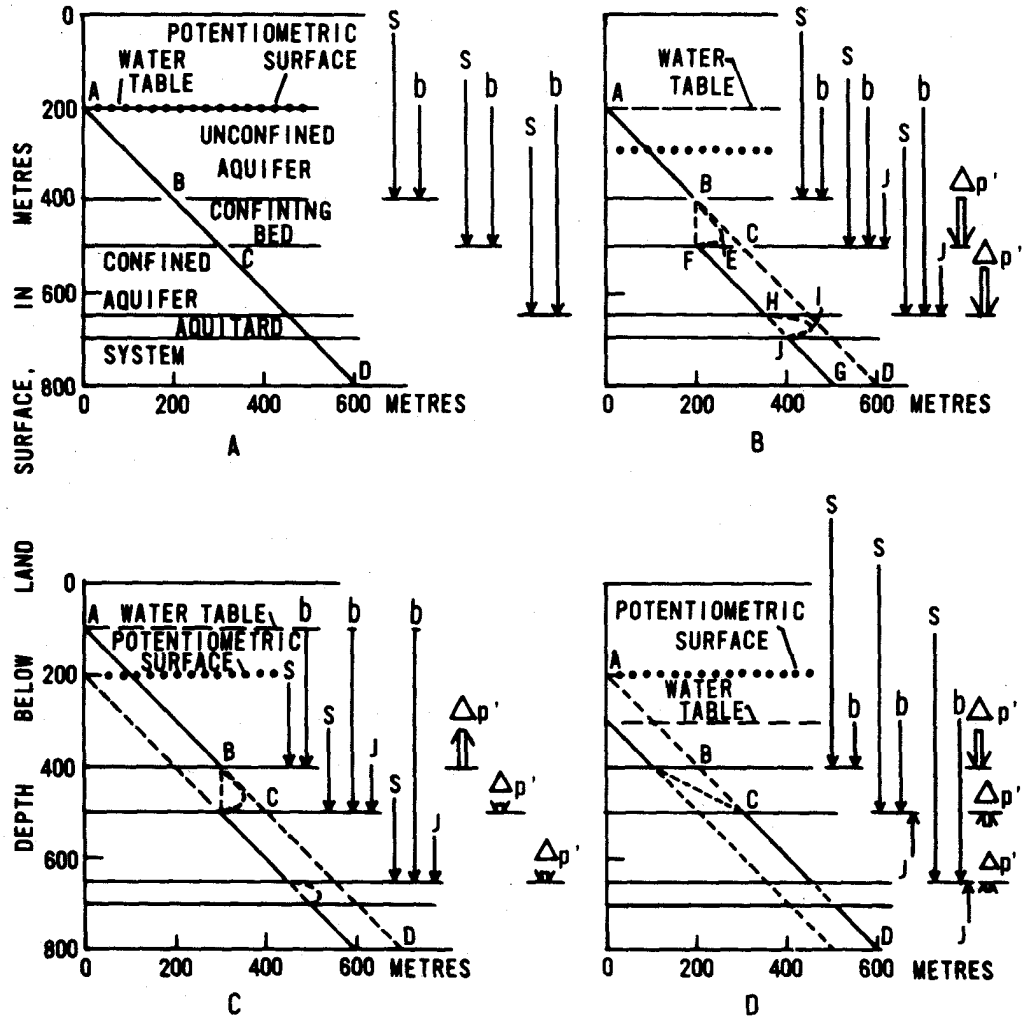

Figure 3.4 Effective stress diagrams for a confined aquifer system overlain by an unconfined aquifer. A, water table and potentiometric surface common. B, water table constant, potentiometric surface lowered. C, water table raised, potentiometric surface constant. D, water table lowered, potentiometric surface constant. Stresses in metres of water; based on assumed porosity = 0.40, specific gravity of solids = 2.7, and specific retention = 0.20. S = effective stress due to weight of unsaturated deposits; b = effective stress due to buoyant weight of submerged deposits; J = seepage stress; $\Delta p'$ = change in total effective stress from condition A.

reference. The effective stress of the saturated deposits increases directly with depth below, the water table, as indicated by the increasing vector lengths, b, at the base of the confining bed and the top of the aquitard.

If the potentiometric surface of the confined aquifer system is drawn down 100 metres as in diagram B, gravitational stresses remain as in A because the water table is unchanged. However, a downward component of hydraulic gradient is developed across the confining bed, which induces downward movement of water through the pores and exerts a viscous drag on the grains. The net force transferred to the grains between any two depths is measured by the head loss between those depths. The stress so exerted on the grains is called a seepage stress. This third effective stress component is represented by vector J on a horizontal plane. Its vertical component is algebraically additive to the gravitational stresses and is transmitted downward through the confined aquifer system. The wide arrows to the right of diagram B indicate within a vertical column the net change in the vertical normal component of effective stress at the base of the confining bed and below, from the hydrostatic condition of diagram A.

Because the water table is unchanged the net change is the change in seepage stress, which is equal to the decrease in fluid (neutral) pressure represented by line C-F (base of confining bed).

The increase in effective stress in the permeable aquifers occurs simultaneously with decrease in head, but decrease of pore pressure in the aquitards and confining beds is delayed because of their high compressibility and low vertical permeability. The reduction in head in the permeable aquifers creates a two-directional hydraulic gradient outward from the center of the aquitard and consequently induces two-directional drainage from the aquitard. Thus, although upward and downward seepage forces occur within the aquitard during this adjustment, internal stresses have no net external effect on the rest of the aquifer system. During this period of transient pressures, the effective stress can increase only as rapidly as the excess pore-pressure decreases. The general pattern of decay is illustrated in diagram B of Figure 3.4 in the confining bed by dashed line B-E-F and in the aquitard by dashed line H-I-J. Full dissipation of excess pore pressures to equilibrium (dashed lines B-F and H-J) may require months or years. Note that water drains through both boundaries of the aquitard, but only through the lower boundary of the confining bed under the specified conditions.

If the potentiometric surface of the confined aquifer system remains constant and the water table is raised or lowered, both gravitational and seepage stresses change, but with opposite sign. For example, if the water table is raised 100 m (diagram C) and the parameters are as assumed earlier, the change in gravitational stress is -0.8 metre of water per metre of rise; however, the unit change in seepage stress (differential between water table and potentiometric surface of confined system) is +1.0 metre. Hence, the net unit change in applied stress in the confined system is +0.2 metre of water. Conversely, if the water table is lowered (diagram D), the net change in applied stress is -0.2 metre per metre of decline.

In summary, water-level fluctuations change effective stresses in the following two ways:

1. A rise of the water table provides buoyant support for the grains in the zone of the change, and a decline removes the buoyant support; these changes in gravitational stress are transmitted downward to all underlying deposits.
2. A change in position of either the water table or the potentiometric surface of the confined aquifer system, or both, may induce vertical hydraulic gradients across confining or semiconfining beds and thereby produce a seepage stress. The vertical normal component of this stress is algebraically additive to the gravitational stress. A change in effective stress results if preexisting seepage stresses are altered in direction or magnitude.

The change in applied stress within a confined aquifer system, due to changes in both the water table and the artesian head, may be summarized concisely (Poland and others, 1972, p. 6) as

$$\Delta p_a = -(\Delta hc - \Delta h_u y_s), \qquad (3.11$$

where p_a is the applied stress expressed in metres of water, h_c is the head (assumed uniform) in the confined aquifer system, h_u is the head in the overlying unconfined aquifer, and y_s is the average specific yield (expressed as a decimal fraction) in the interval of water-table fluctuation.

In the San Joaquin Valley, California, the areas in which subsidence has been appreciable coincide generally with the areas in which ground water is withdrawn chiefly from confined aquifer systems. (See Chapter 9.13, Figure 9.13.2.) Furthermore, the great increases in stress applied to the sediments in the ground-water reservoir by the intensive mining of ground water developed chiefly as increased seepage stresses on the confined aquifer systems.

3.4 COMPRESSIBILITY AND STORAGE CHARACTERISTICS

3.4.1 Stress-strain analysis

Field measurements of compaction and correlative change in water level may serve as continuous monitors of subsidence and indicators of the response of the system to change in applied stress. They also can be utilized to construct stress-strain curves from which, under certain favourable conditions, one can derive storage and compressibility parameters of the aquifer system, as first demonstrated by Riley (1969) for the Pixley site in the southern part of the San Joaquin valley, California.

Thirteen years of measured water-level change and compaction at Pixley are shown in Figure 3.5. They have been utilized to derive a computer plot of stress change versus strain (Figure 3.5, E) for a 101-metre thickness of the confined aquifer system. The change in stress (B) applied to all strata within the depth interval is calculated from the hydrographs (A) of wells 16N4 (water table) and 16N3 (confined system). This stress-change graph is plotted with stress increasing downward to emphasize the close correlation with declining artesian head. The compaction within the 131-232-metre depth interval (D) is obtained as the difference between the two extensometer plots on graph C. The stress-strain diagram (E) represents the mechanica1 response (change in thickness) of the 131-232-metre depth interval to change in effective stress. It is plotted from the calculated data of graphs B and D. For convenience, the stress-change plot of graph B is expressed in equivalent units of water head (1 ft of water head is equivalent to 0.4333 lb in^{-2}; 1 m of head is equivalent to 0.1 kg cm^{-2}).

Attention is directed to (1) the annual depth-to-water pattern for the confined aquifer system (see hydrograph for well 16N3) in response to the characteristic seasonal pumping for irrigation--the main seasonal decline occurs in spring to late summer followed by recovery of water level to a peak late in the winter; (2) the reduced rate of compaction during years of small seasonal drawdown of water level in well 16N3, such as 1962, 1963, 1967 and 1969; (3) the small but definite expansion of the deposits (D) in most winters, accompanying the water-level recovery; and (4) the series of annual stress-strain loops (E), formed by the yearly cycles of stress increase and decrease.

As discussed by Riley (1969):

> "The descending segments of the annual loop are of particular interest since the represent the resultant of two opposing tendencies--one toward continuing compaction and one toward elastic expansion in response to decreasing applied stress. Expansion of the more permeable strata of the aquifer system must be essentially concurrent with the observed rise in head in wells. However, the first reduction of stress may produce only a slight reduction in compaction rate. Evidently, initial expansion of the aquifers is concealed by continuing compaction of the interbedded aquitards as water continues to be expelled under the influence of higher pore pressures remaining within the medial regions of the beds.
>
> "Consolidation theory requires that the maximum excess pore pressure, which is in the middle of a doubly-draining aquitard, be related to the same parameters . . . . . that control the time-consolidation function. It is, therefore, inevitable that there be, at the end of a relatively short pumping season, a large range of maximum excess pore pressures in a sequence of aquitards of widely varying thicknesses and physical properties. Thus, as head in the aquifers rises and stress declines, the thinnest and (or) most permeable aquitards, containing the least excess pore pressure, will quickly assume an elastic response; but the thickest and (or) least permeable beds may continue to compact at diminishing rates through most or perhaps all of the period of head recovery and stress relief.
>
> "Evidence for this type of behavior is contained in the continuously curving stress strain line characteristic of much of the descending portions of the annual loops."

If in Figure 3.5E the lower part of the descending curve approximates a straight line with a positive slope, as it does, for instance, in 1968 and 1970, we can assume that essentially all excess pore pressures have been exceeded by the rising heads and that the entire aquifer system is expanding in accordance with its elastic modulus.

The lower parts of the descending segments of the annual loops for the winters of 1968-69 1969-70, and the latter part of 1970 are approximately parallel straight lines, as shown by the upward projection of the dotted lines. The reciprocal of the slope of the dotted lines is realistic estimate of the component of the storage coefficient, S, attributable, to the elastic or recoverable deformation of the aquifer system skeleton, S_{ke}:

$$S_{ke} = \frac{\Delta b}{\Delta h} = 6.4 \times 10^{-4} \qquad (3.12)$$

where b is the thickness of the aquifer-system segment being measured, Δb is compaction, h is applied stress, and Δh is change in applied stress. The component of average specific storage due to elastic deformation is S_{ske}:

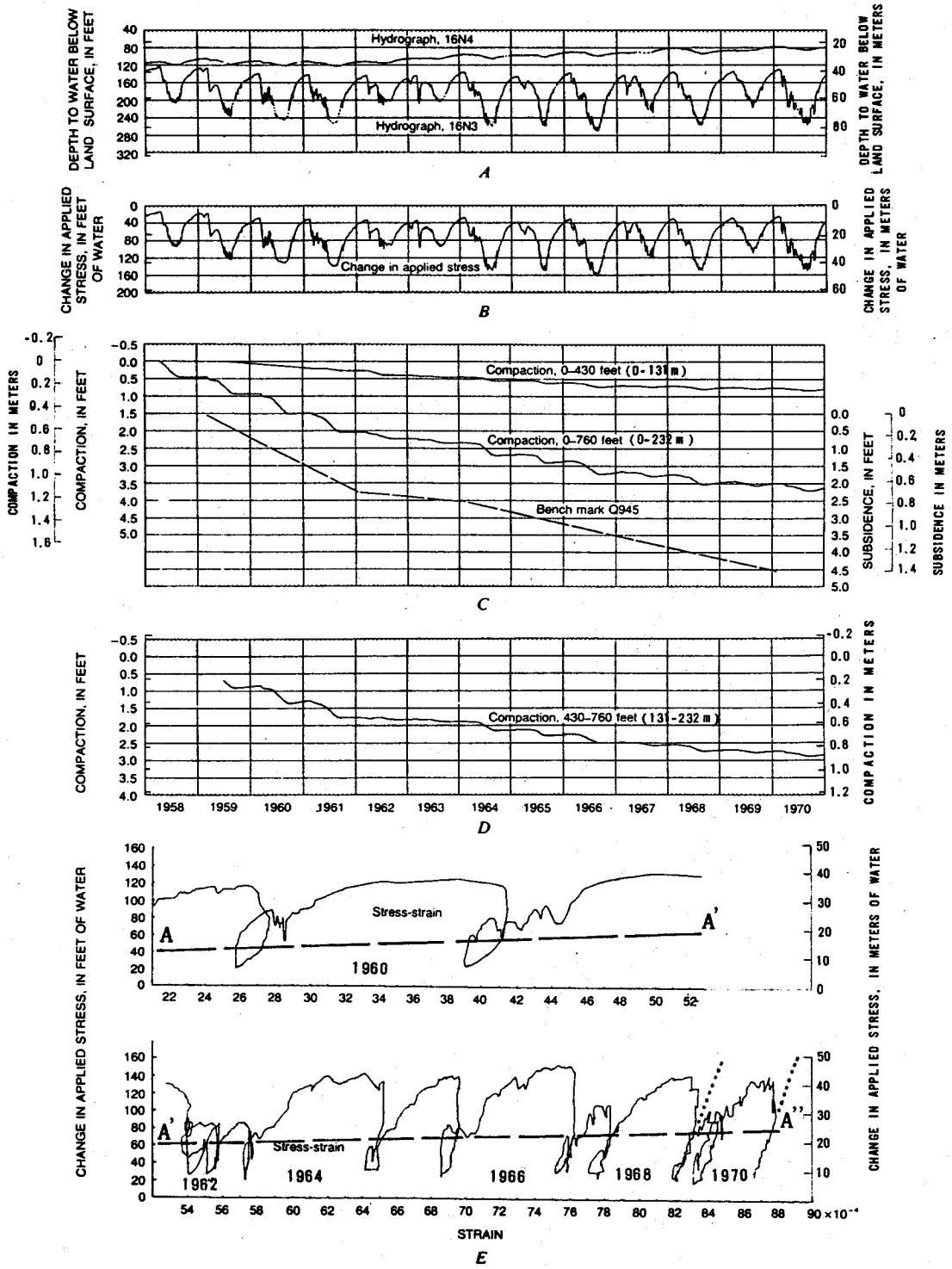

Figure 3.5 Hydrographs, change in applied stress, compaction, subsidence, and stress-strain relationship, 23/25-16N. A, Hydrographs of wells 23/25-16N4, perforated 61-73 m depth, and 23/25-16N3, perforated 110-128 m depth. B, Change in applied stress. C, Compaction to 131-metre depth in well 23/25-16N3 and to 232-metre depth in well 23/25-16N1 and subsidence of bench mark Q945 at well 23/25-16N1. D, Compaction in 131-232-metre depth interval. E, Stress change versus strain (101-metre thickness). (Modified from Poland, Lofgren, Ireland, and Pugh, 1975, Fig. 70.)

$$S_{ske} = \frac{\Delta b}{b} / \Delta h = \frac{S_{ke}}{b} = \frac{6.4 \times 10^{-4}}{101 m} = 6.3 \times (10)^{-6} m^{-1}, \quad (3.13)$$

where $\Delta b/b$ represents strain in Figure 3.5E and can be considered a conservative estimate of bulk volume strain, $\Delta V/V$, in the field. The compressibility of the aquifer-system skeleton in the elastic range of stress is α_{ke}:

$$\alpha_{ke} = \frac{S_{ske}}{\gamma_w} = \frac{6.3 \times 10^{-6} m^{-1}}{0.1 kg cm^{-2} m^{-1}} = 6.3 \times 10^{-5} cm^2 kg^{-1}. \quad (3.14)$$

However, if stresses are expressed in metres of water, and if γ_w (the unit weight of water) equals unity, α_{ke} is equal numerically to S_{ske}. It is of interest to note that the compressibility of water, β_w, at 20° C, is 4.7 x 10^{-5} $cm^2 kg^{-1}$. Hence, the average elastic compressibility of the aquifer-system skeleton is about 1.3 times as large as the compressibility of water.

On the other hand,

$$S_{sw} = n \beta_w \gamma_w, \quad (3.5)$$

If the average porosity, n, equals 0.4, then

$$S_{sw} = (0.4)(4.7 \times 10^{-5} cm^2 kg^{-1})(0.1 kg\ cm^{-2} m^{-l}) = 1.9 \times 10^{-6} m^{-l} \quad (3.15)$$

Therefore, for the 101-metre thickness of the measured interval, the ratio of specific storage values for the elastic deformation of the aquifer system and for the elastic expansion of water is

$$\frac{S_{ske}}{S_{sw}} = \frac{6.3 \times 10^{-6} m^{-1}}{1.9 \times 10^{-6} m^{-1}} = 3.3. \quad (3.16)$$

This means that for each unit of change in head, the volume of water released from or taken into storage per unit volume of the porous medium by elastic (recoverable) deformation of the medium is more than three times the volume released by elastic deformation of the interstitial water

Elastic storage and compressibility parameters have been derived from two other stress-strain plots described in the case histories. One is for a well in western Fresno County, illustrated in Figure 9.13.9. The depth interval measured is 70-176 m below land surface. At this site, S_{ke} = 1.2 x 10^{-3} and S_{ske} = 1.1 x $10^{-5} m^{-1}$. This stress-strain plot (Figure 9.13.9) is of interest also because the lower parts of both the descending and ascending segments of the annual "hysteresis loops" form essentially a common straight line, indicating almost no time delay in adjustment of the aquifer-system skeleton to change in stress in the elastic range of stress.. Of this 106-m thickness of aquifer system, the sum of the aquifers is 71 m or two-thirds of the total and the sum of the aquitards is only one-third of the total. The electric log suggests the aquitards are largely silt and hence relatively permeable compared with clay.

The other plot is for a well in San Jose, California, illustrated in Figure 9.14.7. The depth interval measured is 244 m thick, 61-305 m below the land surface, representing the full thickness of the confined aquifer system. The stress-compaction plot indicates that S_{ke} 1.5 x 10^{-3} and $S_{ske} = S_{ke}/244m$ = 6.15 x $10^{-6} m^{-1}$. In these computations I have assumed that in the range of stresses less than preconsolidation stress, the compressibility of the aquitards and the aquifers is the same. Therefore, the full thickness of the confined aquifer system, 244 m, was used to derive the specific storage component, S_{ske}, in the elastic range of stress.

For stresses exceeding past maximum (preconsolidation) stresses, virgin specific storage and compressibility parameters can be approximated from Figure 3.5. Straight line A-A′-A" is drawn through the annual hysteresis loops approximately at the level at which the rising elastic compaction curve crosses over the descending expansion curve. The reciprocal of the slope of line A-A′-A" is the component of the storage coefficient, S, attributable to the inelastic (nonrecoverable) deformation of the aquifer-system skeleton, S_{kv}:

$$S_{kv} = \frac{\Delta b}{\Delta h} = 6.8 \times 10^{-2} \tag{3.17}$$

The component of specific storage due to inelastic (nonrecoverable) deformation of the aquifer system skeleton is S_{skv}:

$$S_{skv} = \frac{S_{kv}}{b} = \frac{6.8 \times 10^{-2}}{101\text{m}} = 6.7 \times 10^{-4}\text{m}^{-1} \tag{3.18}$$

Relation 3.18 is an average value for the entire system. It is reasonable to assume, however, that only the clay interbeds deform inelastically. To obtain the average nonrecoverable specific storage of the aquitards in accordance with this convention, S_{kv} is divided by the aggregate thickness, b', of aquitards, which is 70 metres:

$$S'_{skv} = \frac{S_{kv}}{b'} = \frac{6.8 \times 10^{-2}}{70\text{m}} = 9.7 \times 10^{-4}\text{m}^{-1} \tag{3.19}$$

The average aquitard compressibility

$$\frac{S'_{skv}}{w} = \frac{9.7 \times 10^{-4}\text{m}^{-1}}{0.1\text{kgcm}^{-2}\text{m}^{-1}} = 9.7 \times 10^{-3}\text{cm}^2\text{kg}^{-1} \tag{3.20}$$

The average compressibility of the aquifer-system skeleton in the virgin range of stressing is α_{kv}:

$$\alpha_{kv} = \frac{S_{skv}}{\gamma_w} = \frac{6.7 \times 10^{-4}\text{m}^{-1}}{0.1\text{kgcm}^{-2}\text{m}^{-1}} = 6.7 \times 10^{-3}\text{cm}^2\text{kg}^{-1} \tag{3.21}$$

Thus, from the appraisal of Figure 3.5, and the comparison of α_{ke} of 3.14 to α_{kv} of 3.21, we can conclude that at Pixley, the compressibility of the measured interval of the aquifer system in the virgin range of stressing is about 100 times as great as the compressibility in the elastic range of stressing. Hydrologists should be aware that in multiaquifer systems the values of the compressibility and storage parameters may be 10 to 100 times greater when total applied stresses are in the virgin range of stressing than when they are in the elastic range. This fact must be kept in mind in the interpretation of aquifer tests and when making estimates of the usable storage capacity of a confined-aquifer system.

3.4.2 Soil-mechanics techniques

Compressibility characteristics of fine-grained compressible layers or lenses (aquitards) can be obtained by making one-dimensional consolidation tests of "undisturbed" cores in the laboratory. These tests are described in soil mechanics textbooks and briefly in Chapter, 4 of this manual. The plot of void ratio against the logarithm of load (effective stress) is known as the e-log p plot. Three parameters that can be obtained from this plot are (1) the compression index, C_c, a measure of the nonlinear compressibility of the sample, (2) the coefficient of consolidation, C_v, a measure of the time rate of consolidation, and (3) the approximate value of the preconsolidation load, determined graphically (see Figure 4-9). The preconsolidation load or stress is the maximum prior effective stress to which a deposit has been subjected and which it can withstand without undergoing additional permanent deformation. Most of the compacting deposits in the subsiding areas of Table 1.1 are of late Cenozoic age and before disturbance of equilibrium conditions by man were normally consolidated or slightly overconsolidated (1 to 4 kg cm^{-2}).

For effective stress changes in the stress range less than preconsolidation stress, the compaction or expansion of both aquitards and aquifers is elastic--that is, approximately proportional to change in effective stress over a moderate range in stress, and fully recoverable if the stress reverts to the initial condition.

For increase in effective stress in the range of loading that exceeds preconsolidation stress, the "virgin" compaction of aquitards is chiefly inelastic--that is, not recoverable upon decrease in stress. However, this virgin compaction includes a recoverable elastic component

that is small compared to the nonrecoverable component. The virgin compaction usually is roughly proportional to the logarithm of effective stress.

The compaction of aquifers, in contrast to that of aquitards, is chiefly elastic (recoverable) but it may include an inelastic component. In poorly sorted and angular sands and especially in micaceous sands, the inelastic component may dominate.

A semilogarithmic plot of void ratio, e, versus the logarithm of load (effective stress p′, shown in Figure 3.6, illustrates a graphic method of computing compressibility. The coefficient of volume compressibility, m_v in soil-mechanics terminology,

$$m_v = \frac{e_0 - e_1}{(1 + e_0)\Delta p'}$$

(Terzaghi and Peck, 1967). It represents the compression of the clay, per unit of initia1 thickness, per unit increase in load (for effective stress change in the range exceeding pre-consolidation stress). Utilizing the laboratory virgin compression curve, which is a straight line on the semilogarithmic plot, we see that for a load change $\Delta p'$, from 100 to 200 lbs in^{-2}

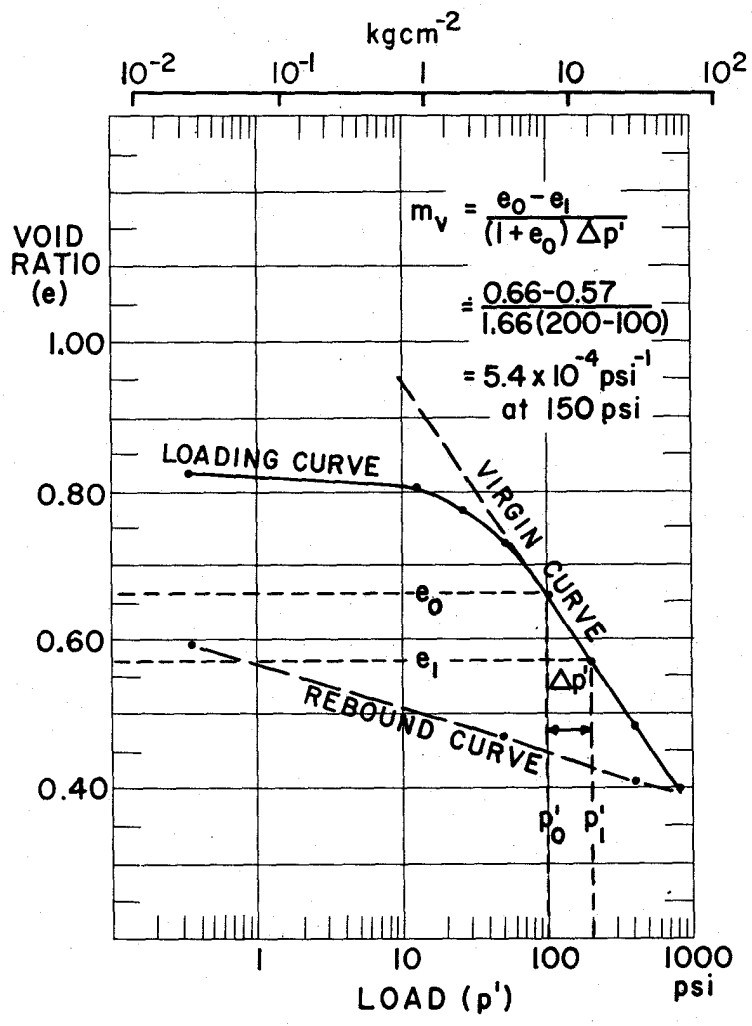

Figure 3.6 Deriving m from e-log p′ plot.

(7 to 14 kg cm^{-2}), the void ratio, e, decreases from 0.66 to 0.57. The decrease in volume or length of the sample, $e_0 - e_1$, divided by the initial volume, $1 + e_0$, and by the change in load for the values given, supplies an approximation of compressibility at the midpoint of $\Delta p'$. Thus, the compressibility at 150 lbs in^{-2} (10.5 kg cm^{-2}) is approximately 5.4×10^{-4} $in^2 lb^{-1}$ (7.7×10^{-3} cm kg^{-1}). The compressibility decreases markedly with increase in effective stress. Repeating the computation, for several increments of load increase furnishes the data for plotting compressibility for the pertinent range in effective stress.

Figure 3.7 is a logarithmic plot showing the principal range in compressibility of tested cores from four core holes tapping alluvial and minor lacustrine deposits in southwestern United States, as well as the compressibility of pure clays made by Chilingar and Knight (1960).

The four core holes are spaced from California to Texas, as follows:

Core hole	Location	Depth (m)
A	Santa Clara Valley, California, in San Jose	305
B	San Joaquin Valley, California, in western Fresno County	610
C	Pinal County, Arizona, near Eloy	592
D	Harris County, Texas, at Clear Lake	294

The graph summarizes the compressibility range for 30 samples from the four core holes for effective stresses between 8 and 100 kg cm^{-2}. If we consider these samples under a common effective stress of 70 kg cm^{-2} (note the vertical dashed line), the range in compressibility of

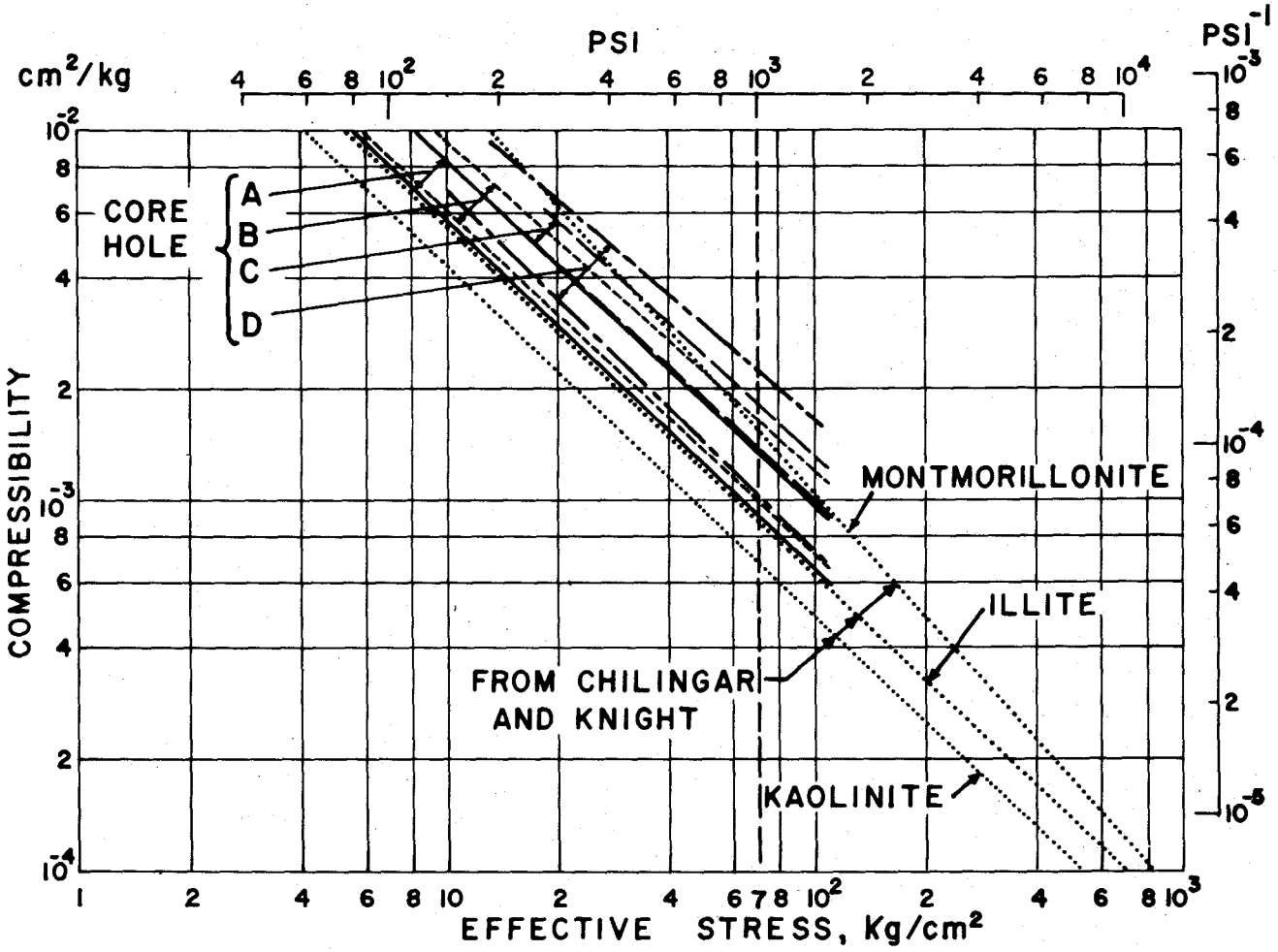

Figure 3.7 Compressibility plots for fine-grained samples from four core holes in southwestern United States and for pure clays tested by Chilingar and Knight (1960).

the 30 cores is about 9 x 10^{-4} to 2.3 x 10^{-3} cm^2 kg^{-1}, a range by a factor of nearly three.

Experimental compaction studies by Chilingar and Knight (1960), made on kaolinite, illite, and montmorillonite clays at pressures from 3 to 14,000 kg cm^{-2} afford an opportunity to compare compressibilities of the fine-grained corehole samples with those of pure clays. The standard clay-mineral samples tested were described by Chilingar and Knight (1960, p. 103) as follows:

Montmorillonite No. 25, Upton, Wyoming
Illite No. 35, Fithian, Illinois
Kaolinite No. 4, Macon, Georgia

The results of their tests, which they expressed in moisture content in per cent (dry weight) versus the logarithm of pressure, have been converted to compressibility versus effective stress and are shown as dotted lines in Figure 3.7. Kaolinite has the lowest compressibility, illite the intermediate, and montmorillonite has the highest. The compressibilities of all 30 corehole samples are higher than those of the standard illite throughout the stress range tested. Furthermore, the compressibilities of all the samples from core holes A and B (central California) fall between the standard illite and montmorillonite curves. X-ray diffraction analysis of the clay-mineral assemblages at all four sites indicated that montmorillonite is the predominant clay mineral, ranging from 6 to 8 parts in 10.

Compressibility tests have been made on many samples of fine-grained sediments taken from a deep (950m) borehole in Venice, Italy, in 1971. Values of m_v versus depth for more than 50 samples are plotted in Figure 9.3.3 of the Venice case history. The compressibilities were computed at the actual "in situ" pressures for both the loading and unloading curves. Ricceri and Butterfield (1974) made a detailed analysis of the compressibility data from the deep borehole. If the compressiblities for samples from 120-220 m depth, computed from the loading curve (m_{vl} points in Figure 9.3.3), are plotted in Figure 3.7, most points fall on or just to the right of the illite curve. Compressibilities average about 3 x 10^{-3} cm^2kg^{-1} for effective stresses in the range of 12 to 22 kg cm^{-2} (120-220 m depth). The highest compressibilities fall within the range of compressibilities for samples from corehole A (Santa Clara Valley, Calif.).

3.4.3 The compressibility environment

Effective stresses, including the increase applied by pumping, are in the range of 10 to 100 kg cm^{-2} for aquifer systems tapped by water wells within depths of 60 to 900 m. This depth range includes about all the stressed sediments of Table 1.1. Within this stress range sands in general are much less compressible than clays. However, at effective stresses of 100 to 200 kg cm^{-2}, evidence is accumulating to show that some sands may be as compressible as clays or siltstones.

Roberts (1969) made a laboratory study of the compressiblity of sands and clays as determined from one-dimensional consolidation tests at stresses up to 700 kg cm^{-2}. The tests showed that in the range of effective stresses from 100 to 200 kg cm^{-2}, some sands were as compressible as typical clays. Roberts noted that sands are relatively incompressible at low pressures (<100 kg cm^{-2})--the compression is due to particle rearrangement. At higher pressures fracturing of the grains develops. He concluded that factors affecting the pressures at which fracturing begins include the initial density of the sample, angularity of the grains, and grain-size distribution.

In a study of subsidence of oil fields bordering Lake Maracaibo in Venezuela, van der Knapp and van der Vlis (1967) made one-dimensional consolidation tests on cores of uncemented sand and clay, taken from depths of 900 to 1050 m. Compressibility was computed from the virgin compression curve of the e-log p’ plot. The composite graphs of compressibility of the sand and clay samples showed that the two materials have comparable compressibilities. For example, at 140 kg cm^{-2} of effective stress, the mean sand compressibility (8 samples) is about 5.7 x 10^{-4} cm kg^{-1} and the mean clay compressibility (11 samples) is about 4.5 x 10^{-4} cm^2kg^{-1}.

The principal oil zones at the Wilmington oil field in Los Angeles and Long Beach, California, that compacted to cause as much as 9 m of subsidence are at depths of 600 to 1200 m. When fluid pressures in the zones were depleted in the late 1950’s prior to repressuring, effective stresses were 100 to 200 kg cm^{-2} According to Allen and Mayuga (1969), axial loading tests on the reservoir sands and siltstones showed the sands to be as compactible, or more so, than the siltstones at the field effective stresses. From the laboratory tests, reservoir calculations, and casing-collar measurements, they concluded that about two-thirds of the compaction

had occurred in the sands and one-third in the siltstones. The sands are composed of about 35-70 per cent quartz, 12-40 per cent feldspar, and 8-12 per cent silt and clay minerals. Above the 1,220 m depth, the sands are uncemented and loose, and they grade in grain size from fine to coarse. Roberts' (1969) findings that some sands fracture appreciably in the stress range of 100-200 kg cm^{-2} suggest that the high compressibility of the feldspathic Wilmington "oil sands" in this same effective-stress range is due chiefly to fracturing.

For additional information on the compressibilities of unconsolidated sands and clays, the reader is referred to Roberts (1969), Meade (1968), Grim (1962), Allen and Chilingarian, in Chilingarian and Wolf (1975, p. 43-77), and Rieke and Chilingarian (1974, p. 173-217).

3.5 REFERENCES

ALLEN, D. R., and MAYUGA, M. N. 1969. The mechanics of compaction and rebound, Wilmington oil field, Long Beach, California, USA, in L. J. Tison, ed., Land Subsidence, v. 2, Internat. Assoc. Sci. Hydrology Pub. 89, p. 410-422.

CHILINGAR, G. V., and KNIGHT, LARRY. 1960. Relationship between pressure and moisture content of kaolinite, illite, and montmorillonite clays. Bull. Am. Assoc. Petroleum Geologists, v. 44, no. 1, p. 101-106.

CHILINGARIAN, G. V., and WOLF, K. H., eds. 1975. Compaction of coarse-grained sediments, I. Elsevier Scientific Publishing Company, Amsterdam, 552 p.

FERRIS, J. G., KNOWLES, D. B., BROWN, R. H., and STALLMAN, R. W. 1962. Theory of aquifer tests. U.S. Geol. Survey Water-Supply Paper 1536-E, p. 69-174.

GRIM, R. E. 1962. Applied clay mineralogy. McGraw-Hill Book Company, Inc. New York, 422 p.

HELM, D. C. 1978. A postulated relation between granular movement and Darcy's law for transient flow. Proceedings of Conference on Evaluation and Prediction of Subsidence, S. K. Saxena, ed., American Soc. Civil Engineers, p. 417-440.

HELM, D. C. 1982. Conceptual aspects of subsidence due to fluid withdrawal, in Recent trends in hydrogeology, Geological Society of America Special Paper in press.

JACOB, C. E. 1940. On the flow of water in an elastic artesian aquifer. Am. Geophys. Union Trans., pt. 2, p. 574-586.

LOFGREN, B. E. 1968. Analysis of stresses causing land subsidence. U.S. Geol. Survey Prof. Paper 600-B, p. B219-B225.

LOHMAN, S. W., and others. 1972. Definitions of selected ground-water terms--Revisions and conceptual refinements. U.S. Geol. Survey Water-supply Paper 1978, 21 p.

MAYUGA, M. N., and ALLEN, D. R. 1969. Subsidence in the Wilmington oil field, Long Beach, Calif., USA, in L. J. Tison, ed., Land subsidence, v. 1. Internat. Assoc. Sci. Hydrology Pub. 88, p. 6C6-79.

MEADE, R. H. 1968. Compaction of sediments underlying areas of land subsidence in central California. U.S. Geol. Survey Prof. Paper 497-D, 39 p.

MEINZER, 0. E. 1923. outline of ground-water hydrology with definitions. U.S. Geol. Survey Water-Supply Paper 494, 71 p.

MEINZER, 0. E. 1928. Compressibility and elasticity of artesian aquifers. Econ. Geology, v. 23, no. 3, p. 263-291.

MEINZER, 0. E., and HARD, H. A. 1925. The artesian-water supply of the Dakota sandstone in North Dakota with special reference to the Edgeley quadrangle. U.S. Geol. Survey Water-Supply Paper 520-E, p. 73-95.

POLAND, J. P. 1972. Subsidence and its control. Am. Assoc. Petroleum Geologists Underground Waste Management and Environmental implications, Memoir No. 18, p. 50-71.

POLAND, J. F., and DAVIS, G. H. 1969. Land subsidence due to withdrawal of fluids, in Varnes, D. J., and Kiersch, G., eds. Reviews in engineering geology, v. 2. Geol. Soc. America, p. 187-269.

POLAND, J. P., LOFGREN, B. E., IRELAND, R. L., and PUGH, R. G., 1975. Land subsidence in the San Joaquin Valley, California, as of 1972. U.S. Geol. Survey Prof. Paper 437-H, 77 p.

POLAND, J. F., LOFGREN, B. E., and RILEY, F. S., 1972. Glossary of selected terms useful in the studies of the mechanics of aquifer systems and land subsidence due to fluid withdrawal. U.S. Geol. Survey Water-Supply Paper 2025, 9 p.

RICCERI, G., and BUTTERFIELD, R. 1974. An analysis of compressibility data from a deep borehole in Venice. Geotechnique, no. 2, p. 175-192.

RIEKE, H. H., III, and CHILINGARIAN, G. V. 1974. Compaction of argillaceous sediments. Elsevier Scientific Publishing Company, Amsterdam, 424 p.

RILEY, F. S. 1969. Analysis of borehole extensometer data from central California, in Tison, L. J., ed., Land subsidence, v. 2. Internat. Assoc. Sci. Hydrology Pub. 89, p. 423-431.

ROBERTS, J. E. 1969. Sand compression as a factor in oil field subsidence, in Tison, L.J., ed., Land subsidence, v. 2. Internat. Assoc. Sci. Hydrology Pub. 89, p. 368-376.

SCOTT, R. F. 1963. Principles of soil mechanics. Addison-Wesley Pub. Co., Palo Alto, California, 550 p.

TAYLOR, D. W. 1948. Fundamentals of soil mechanics. New York, John Wiley and Sons, Inc., 700 p

TERZAGHI, KARL. 1925. Principles of soil mechanics: IV, Settlement and consolidation of clay. Eng. News-Rec., p. 874-878.

TERZAGHI, KARL, and PECK, R. B. 1967. Soil mechanics in engineering practice. New York, John Wiley and Sons, Inc. 2d ed., 729 p.

THEIS, C. V. 1935. The relation between the lowering of the piezometric surface and the rate and duration of discharge of a well using ground-water storage. Am. Geophys. Union Trans., v. 16, p. 519-524.

THEIS, C. V. 1938. The significance and nature of the cone of depression in ground-water bodies. Econ. Geology, v. 33, no. 8, p. 889-902.

VAN DER KNAPP, W., and VAN DER VLIS, A. C. 1967. On the cause of subsidence in oil-producing area, in Drilling and production. Mexico City, 7th World Petroleum Cong. Proc., v. 3, p. 85-95.